Article

Ruthenium(II)-Catalyzed Hydrogenation of Carbon Dioxide to Formic Acid. Theoretical Study of Real Catalyst, Ligand Effects, and Solvation Effects

Yu-ya Ohnishi, Tadashi Matsunaga, Yoshihide Nakao, Hirofumi Sato, and Shigeyoshi Sakaki

J. Am. Chem. Soc., **2005**, 127 (11), 4021-4032• DOI: 10.1021/ja043697n • Publication Date (Web): 23 February 2005

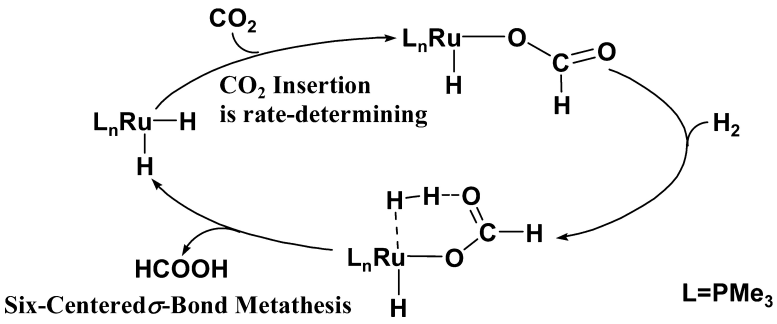

More About This Article

Additional resources and features associated with this article are available within the HTML version:

- Supporting Information
- Links to the 11 articles that cite this article, as of the time of this article download
- Access to high resolution figures
- Links to articles and content related to this article
- Copyright permission to reproduce figures and/or text from this article

View the Full Text HTML

J|A|C|S
ARTICLES
Published on Web 02/23/2005

Ruthenium(II)-Catalyzed Hydrogenation of Carbon Dioxide to Formic Acid. Theoretical Study of Real Catalyst, Ligand Effects, and Solvation Effects

Yu-ya Ohnishi, Tadashi Matsunaga, Yoshihide Nakao, Hirofumi Sato, and Shigeyoshi Sakaki*

Contribution from the Department of Molecular Engineering, Graduate School of Engineering, Kyoto University, Nishikyo-ku, Kyoto 615-8510, Japan

Received October 16, 2004; E-mail: sakaki@moleng.kyoto-u.ac.jp

Abstract: Ruthenium-catalyzed hydrogenation of carbon dioxide to formic acid was theoretically investigated with DFT and MP4(SDQ) methods, where a real catalyst, *cis*-$Ru(H)_2(PMe_3)_3$, was employed in calculations and compared with a model catalyst, *cis*-$Ru(H)_2(PH_3)_3$. Significant differences between the real and model systems are observed in CO_2 insertion into the Ru(II)−H bond, isomerization of a ruthenium(II) η^1-formate intermediate, and metathesis of the η^1-formate intermediate with a dihydrogen molecule. All these reactions more easily occur in the real system than in the model system. The differences are interpreted in terms that PMe_3 is more donating than PH_3 and the trans-influence of PMe_3 is stronger than that of PH_3. The rate-determining step is the CO_2 insertion into the Ru(II)−H bond. Its $\Delta G^{\circ\ddagger}$ value is 16.8 (6.8) kcal/mol, where the value without parentheses is calculated with the MP4(SDQ) method and that in parentheses is calculated with the DFT method. Because this insertion is considerably endothermic, the coordination of the dihydrogen molecule with the ruthenium(II)-η^1-formate intermediate must necessarily occur to suppress the deinsertion. This means that the reaction rate increases with increase in the pressure of dihydrogen molecule, which is consistent with the experimental results. Solvent effects were investigated with the DPCM method. The activation barrier and reaction energy of the CO_2 insertion reaction moderately decrease in the order gas phase > *n*-heptane > THF, while the activation barrier of the metathesis considerably increases in the order gas phase < *n*-heptane < THF. Thus, a polar solvent should be used because the insertion reaction is the rate-determining step.

Introduction

Hydrogenation of carbon dioxide is one of the important and attractive subjects of research in recent transition-metal chemistry, catalytic chemistry, and organometallic chemistry.[1] This reaction was very previously carried out by Inoue and his collaborators in 1976,[2] while the turnover numbers reported were very small. In 1992 to 1994, several important studies were reported,[3−6] to our understanding. Tsai and Nicholas carried out the hydrogenation of carbon dioxide with $[Rh(NBD)(PMe_2Ph)_3]BF_4$ (NBD = norbornadiene).[3] They spectroscopically observed rhodium(III) hydride and rhodium(III) formate complexes such as $[Rh(H)_2(PMe_2Ph)_3(S)]BF_4$ (S = H_2O or THF), $[Rh(H)(PMe_2Ph)_2(\eta^2\text{-}O_2CH)]BF_4$, and $[Rh(H)(S)_n(PMe_2Ph)_{3-n}(\eta^1\text{-}O_2CH)]BF_4$ in the reaction solution. Based on their observation, they proposed that the hydrogenation reaction took place through insertion of carbon dioxide into the Rh(III)−H bond followed by reductive elimination of formic acid and oxidative addition of dihydrogen molecule to the Rh(I) center. Leitner and his collaborators succeeded in the hydrogenation of carbon dioxide with a rhodium(I) hydride complex, $Rh(H)(diphos)_2$ (diphos = 1,2-bis(diphenylphosphino)ethane or 1,3-bis(diphenylphosphino)propane), as a catalyst.[4] In this reaction, a slightly different reaction mechanism was theoretically proposed by Hutschka et al.,[5] which consisted of insertion of carbon dioxide into the Rh(I)−H bond followed by metathesis of the rhodium(I) η^1-formate complex with a dihydrogen molecule. Jessop, Ikariya, and Noyori also succeeded in the ruthenium(II)-catalyzed hydrogenation of carbon dioxide.[6] This catalytic reaction is of particular importance because of the extremely high turnover numbers. From theoretical study, Musashi and Sakaki reported that this reaction took place through insertion of carbon dioxide into the Ru(II)−H bond and isomerization of a ruthenium(II) η^1-formate intermediate followed by metathesis of the ruthenium(II) η^1-formate intermediate with dihydrogen molecule, as shown in

(1) (a) Braunstein, P.; Matt, D.; Nobel, D. *Chem. Rev.* **1988**, *88*, 747. (b) Behr, A. *Angew. Chem., Int. Ed. Engl.* **1988**, *27*, 661. (c) Jessop, P. G.; Ikariya, T.; Noyori, R. *Chem. Rev.* **1995**, *95*, 259. (d) Darensbourg, D. J.; Holtcamp, M. W. *Coord. Chem. Rev.* **1996**, *153*, 155. (e) Walther, D.; Rubens, M.; Rau, S. *Coord. Chem. Rev.* **1999**, *182*, 67.
(2) Inoue, Y.; Izumida, H.; Sasaki, S.; Hashimoto, H. *Chem. Lett.* **1976**, 863. Sasaki, S.; Inoue, Y.; Hashimoto, H. *J. Chem. Soc., Chem. Commun.* **1976**, 605.
(3) Tsai, J. C.; Nicholas, K. H. *J. Am. Chem. Soc.* **1992**, *114*, 5117.
(4) (a) Graf, E.; Leitner, W. *J. Chem. Soc., Chem. Commun.* **1992**, 623. (b) Burgemeister, T.; Kasmer, F.; Leitner, W. *Angew. Chem., Int. Ed. Engl.* **1993**, *32*, 739. (c) Gassner, F.; Leitner, W. *J. Chem. Soc., Chem. Commun.* **1993**, 1465.
(5) (a) Hutschka, F.; Dedieu, A.; Eichberger, M.; Fornika, R.; Reitner, W. *J. Am. Chem. Soc.* **1997**, *119*, 4432. (b) Hutschka, F.; Dedieu, A. *J. Chem. Soc., Dalton Trans.* **1997**, 1899.
(6) (a) Jessop, P. G.; Ikariya, T.; Noyori, R. J. *Nature* **1994**, *368*, 231. (b) Jessop, P. G.; Hsiao, Y.; Ikariya, T.; Noyori, R. *J. Am. Chem. Soc.* **1994**, *116*, 8851. (c) Jessop, P. G.; Ikariya, T.; Noyori, R. *J. Am. Chem. Soc.* **1996**, *118*, 344.

Scheme 1

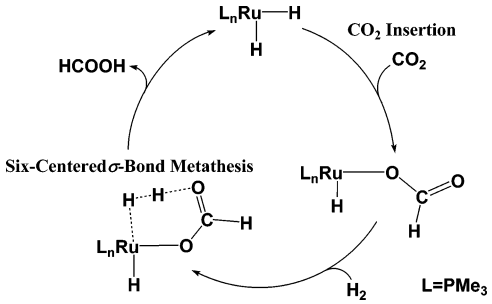

Scheme 1.[7] The same authors also reported that the rhodium(III)-catalyzed hydrogenation of carbon dioxide took place via the insertion of carbon dioxide into the Rh(III)−H bond followed by the reductive elimination of formic acid,[8] as experimentally proposed.[3] From these results of theoretical studies,[5,7−9] it is likely to consider that the reaction mechanism of transition-metal-catalyzed hydrogenation of carbon dioxide has been clearly elucidated. However, there remain important issues to be investigated theoretically. One of them is the rate-determining step in the ruthenium(II)-catalyzed hydrogenation of carbon dioxide. The dependence of the reaction rate on the pressure of dihydrogen molecule[6] suggests that the dihydrogen molecule participates in the rate-determining step. However, the theoretical study previously reported that the rate-determining step was the insertion of carbon dioxide into the Ru(II)−H bond.[7] This seeming discrepancy should be investigated in detail, because the difference in rate-determining step suggests the possibility that the theoretical study did not present correct results of the reaction mechanism. The next is solvent effects; although previous theoretical studies were carried out without consideration of solvent effects, the polarity of solvent is expected to influence the insertion of carbon dioxide into the metal−hydride bond and the metathesis of the metal-η^1-formate intermediate with dihydrogen molecule because their transition states are polarized. Also, not a real catalyst *cis*-$Ru(H)_2(PMe_3)_3$ but a model catalyst *cis*-$Ru(H)_2(PH_3)_3$ was employed in the previous theoretical works.[7,8] It is likely to consider that the computational results with a model system deviate from the correct features.

In this work, we theoretically investigated the ruthenium(II)-catalyzed hydrogenation of carbon dioxide into formic acid, where the real catalyst, *cis*-$Ru(H)_2(PMe_3)_3$, was employed in calculations and solvent effects were taken into consideration. Comparison between *cis*-$Ru(H)_2(PMe_3)_3$ and the PH_3 analogue provides us the knowledge of ligand effects in this catalytic reaction because PH_3 is considered a model of a weakly electron-donating ligand such as phosphite but PMe_3 is a typical donating ligand. Our purposes here are to present detailed knowledge of each elementary process, ligand effects, and solvent effects and to provide theoretical answers about the rate-determining step and the pressure effects of the dihydrogen molecule. We wish to report the conclusive discussion on these issues.

Computations

Geometries were optimized with the DFT method, where the B3LYP functional was used for the exchange-correlation term.[10,11] We ascertained that each optimized transition state exhibited one imaginary frequency and that the geometry changes induced by the imaginary frequency accorded with the reaction course (see Supporting Information Table S1 for geometries of intermediates and transition states). Energy and population changes were calculated with the DFT and MP2 to MP4(SDQ) methods. Solvation effects were evaluated with the DPCM method.[12]

Two kinds of basis set systems were used. The smaller system (BS-I) was employed in geometry optimization. In this BS-I system, core electrons of Ru (up to 3d) and P (up to 2p) were replaced with effective core potentials (ECPs), where (341/321/31) and (21/21/1) basis sets were employed for valence electrons of Ru[13] and P,[14,15] respectively. A 6-311G basis set augmented with a p-polarization function was employed for the hydride ligand, the dihydrogen molecule, and the H atom of formate, where a usual 6-31G basis set was employed for the other H atoms.[16] For C and O, usual 6-31G(d) basis sets were employed.[17] The better basis set system (BS-II) was employed in evaluation of energy and population changes. In the BS-II system, a (541/541/211/1) basis set was used to represent valence electrons of Ru,[18,19] where the same ECPs as those of BS-I were employed for its core electrons. For C, O, and H, the 6-311+G(d) basis sets were used, while the usual 6-31G(d) basis sets were employed for the Me group of PMe_3. For P, the same basis set and ECPs as those of BS−I were used.

As will be shown below, the ruthenium(II) dihydride complex and ruthenium(II) η^1-formate complex form adducts with carbon dioxide and the dihydrogen molecule, respectively, in the catalytic cycle. In such processes, entropy effects should be taken into consideration. We evaluated entropy in two ways. In one way, translation, rotation, and vibration movements were considered to evaluate entropy and thermal energy, where all substrates were treated as ideal gas. The DFT/BS-I method was adopted to calculate vibration frequencies without a scaling factor. In the other way, vibration movements were considered in evaluation of entropy but neither translation movements nor rotation ones were considered, since this reaction was carried out in supercritical carbon dioxide solvent in which the translation and rotation movements are considerably suppressed, compared to those in ideal gas. The free energy change estimated in this way is named $\Delta G_v°$ hereafter. In the former estimation way, entropy significantly decreases when two molecules form an adduct, as expected. In the latter estimation way, on the other hand, entropy change is small, as will be discussed below. The former method apparently overestimates the entropy change and the thermal energy change of solution reaction, because translation and rotation movements are highly suppressed in solution. On the other hand, the latter one underestimates the entropy change and the thermal energy change because translation and rotation movements are not completely frozen in solution. A true value of free energy change would be intermediate between the $\Delta G°$ value evaluated by the former method and the $\Delta G_v°$ value by the latter one. Because this ambiguity remains in the estimation of entropy change and thermal energy change, we

(7) Musashi, Y.; Sakaki, S. *J. Am. Chem. Soc.* **2000**, *122*, 3867.
(8) Musashi, Y.; Sakaki, S. *J. Am. Chem. Soc.* **2002**, *124*, 7588.
(9) Sakaki, S.; Musashi, Y. In *Catalysis by Metal Complexes Vol. 25, Computational Modeling of Homogeneous Catalysis*; Maseras, F., Lledos, A., Eds.; Kluwer Academic Publishers: Dordrecht, 2002; p 79.
(10) (a) Becke, A. D. *Phys. Rev. A*, **1988**, *38*, 3098. (b) Becke, A. D. *J. Chem. Phys.* **1983**, *98*, 5648.
(11) Lee, C.; Yang, W.; Parr, R. G. *Phys. Rev. B* **1988**, *37*, 785.
(12) (a) Miertus, S.; Scrocco, E.; Tomasi, J. *Chem. Phys*. **1981**, *55*, 117. (b) Pascual-Ahuir, J. L.; Silla, E.; Tomasi, J.; Bonaccorsi, R. *J. Comput. Chem.* **1987**, *8*, 778. (c) Floris, F.; Tomasi, J. *J. Comput. Chem.* **1989**, *10*, 616. (d) Tomasi, J.; Persico, M. *Chem. Rev.* **1994**, *94*, 2027.
(13) Hay, P. J.; Wadt, W. R. *J. Chem. Phys.* **1985**, *82*, 299.
(14) Wadt, W. R.; Hay, P. J. *J. Chem. Phys.* **1985**, *82*, 284.
(15) Höllwarth, A.; Böhme, M.; Dapprich, S.; Ehlers, A. W.; Gobbi, A.; Jonas, V.; Köhler, K. F.; Stegmann, R.; Veldkamp, A.; Frenking, G. *Chem. Phys. Lett.* **1993**, *208*, 237.
(16) Krishnan, R.; Binkley, J. S.; Seeger, R.; Pople, J. A. *J. Chem. Phys*. **1980**, *72*, 650.
(17) Hehre, W. J.; Ditchfield, R.; Pople, J. A. *J. Chem. Phys*. **1972**, *56*, 2257.
(18) Couty, M.; Hall, M. B. *J. Comput. Chem*. **1996**, *17*, 1359.
(19) Ehlers, A. W.; Böhme, M.; Dapprich, S.; Gobbi, A.; Höllwarth, A.; Jonas, V.; Köhler, K. F.; Stegmann, P.; Veldkamp, A.; Frenking, G. *Chem. Phys. Lett.* **1993**, *208*, 111.

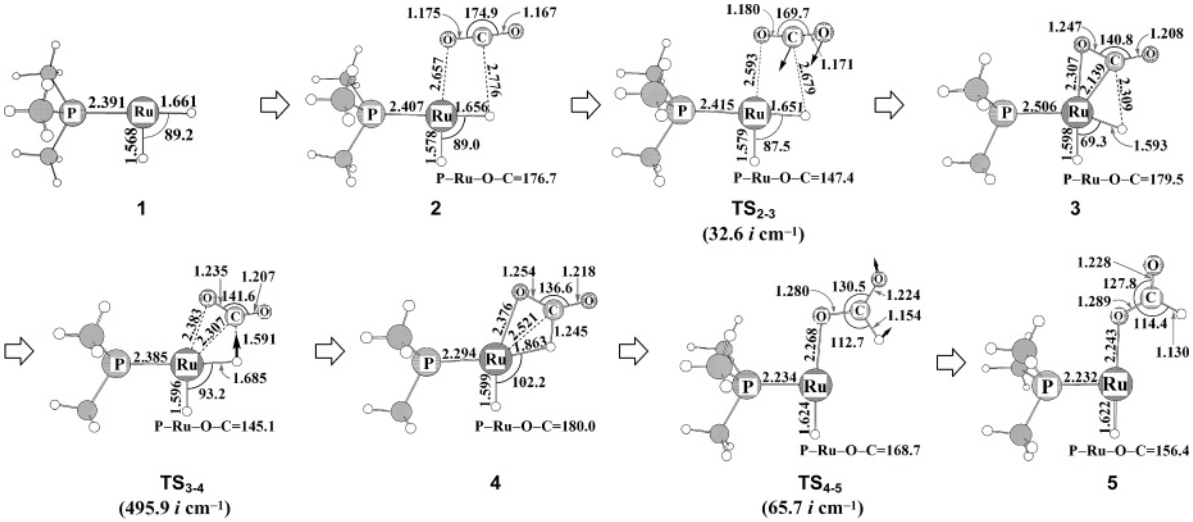

Figure 1. Geometry changes by the insertion of carbon dioxide into the Ru(II)−H bond of *cis*-Ru(H)$_2$(PMe$_3$)$_3$ (two PMe$_3$ ligands in front of and behind the Ru center are omitted in all the figures to show clearly the geometry changes by the reaction). Bond length in angstrom and bond angle in degree. In parentheses is imaginary frequency of each transition state. Arrows in **TS$_{2-3}$** and **TS$_{3-4}$** represent geometry changes involved in each imaginary frequency.

will discuss each elementary step with the usual potential energy changes and then discuss it with the free energy changes evaluated by these two ways.

Gaussian 98 program package was used for these calculations.[20] Population analysis was carried out with the method of Weinhold et al.[21] A contour map of molecular orbitals was drawn with the MOLEKEL program package.[22]

Results and Discussion

Insertion of Carbon Dioxide into the Ru(II)−H Bond: Carbon dioxide approaches the empty coordination site of *cis*-Ru(H)$_2$(PMe$_3$)$_3$ **1**, to afford a reactant complex, *cis*-Ru(H)$_2$(PMe$_3$)$_3$(CO$_2$) **2**, as shown in Figure 1, in which two PMe$_3$ ligands exist in front of and behind the Ru center, respectively, but they are omitted for brevity in all figures. In **2**, the Ru−O and C−O distances are 2.657 and 2.776 Å, respectively, and the OCO angle slightly decreases by about 5°. These geometrical features indicate that carbon dioxide weakly interacts with the Ru center. Starting from **2**, carbon dioxide further approaches the Ru center through the transition state **TS$_{2-3}$**, to afford an intermediate, *cis*-Ru(H)$_2$(PMe$_3$)$_3$(η^2-CO$_2$) **3**. Carbon dioxide has not been inserted into the Ru(II)−H bond in **3**, because the C−H distance between the H ligand and carbon dioxide is still very long (2.309 Å) in **3**. Thus, **3** is characterized as a ruthenium(II) complex of carbon dioxide. Actually, the geometrical features of **3** agree well with those of the usual transition-metal carbon dioxide complexes with a η^2-coordination structure;[23−26] for instance, the OCO angle considerably decreases to 141°, the C=O double bond that coordinates with the Ru center somewhat lengthens to 1.247 Å by 0.08 Å, and the Ru−C distance is considerably shorter than the Ru−O distance in **3**. These geometrical features are easily interpreted in terms of the charge-transfer (CT) interaction between the π^* orbital of carbon dioxide and the doubly occupied d_π orbital of the Ru center, as follows: Because the Ru(II) atom takes a d^6 electron configuration in **3**, the d_π orbital mainly contributes to the HOMO of *cis*-Ru(H)$_2$(PMe$_3$)$_3$, which overlaps well with the π^* orbital of CO$_2$ in a bonding way, as shown in Figure 2A. This CT interaction increases the electron population of the π^* orbital, which lengthens the C−O bond and decreases the O−C−O angle. The shorter Ru−C bond than the Ru−O bond results from the fact that the p orbital of the C atom contributes more to the π^* orbital of CO$_2$ than does that of the O atom.

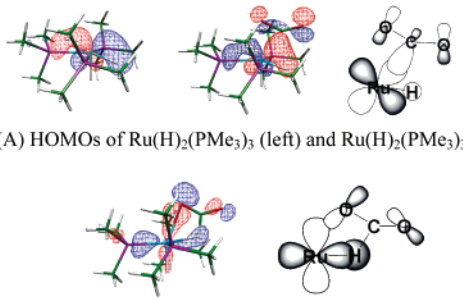

(A) HOMOs of Ru(H)$_2$(PMe$_3$)$_3$ (left) and Ru(H)$_2$(PMe$_3$)$_3$(CO$_2$) (right)

(B) Agostic interaction between the C-H bond of formate and d_σ orbital of Ru

Figure 2. Several important orbitals in *cis*-Ru(H$_2$)(PMe$_3$)$_3$(CO$_2$) and Ru(H)(η^1-OCOH)(PMe$_3$)$_3$ (two PMe$_3$ ligands in front of and behind the Ru center are omitted in all the figures to show clearly the geometry changes by the reaction). The wave function surface with the value of 0.05e is plotted.

The next step is the insertion of carbon dioxide into the Ru(II)−H bond, which takes place through the transition state

(20) Frisch, M. J.; Trucks, G. W.; Schlegel, H. B.; Scuseria, G. E.; Robb, M. A.; Cheeseman, J. R.; Zakrzewski, V. G.; Montgomery, J. A.; Stratmann, R. E.; Burant, J. C.; Dapprich, S.; Millam, J. M.; Daniels, A. D.; Kudin, K. N.; Strain, M. C.; Farkas, O.; Tomasi, J.; Barone, V.; Cossi, M.; Cammi, R.; Mennucci, B.; Pomelli, C.; Adamo, C.; Clifford, S.; Ochterski, J.; Petersson, G. A.; Ayala, P. Y.; Cui, Q.; Morokuma, K.; Malick, D. K.; Rabuck, A. D.; Raghavachari, K.; Foresman, J. B.; Cioslowski, J.; Ortiz, J. V.; Stefanov, B. B.; Liu, G.; Liashenko, A.; Piskorz, P.; Komaromi, I.; Gomperts, R.; Martin, R. L.; Fox, D. J.; Keith, T.; Al-Laham, M. A.; Peng, C. Y.; Nanayakkara, A.; Gonzalez, C.; Challacombe, M.; Gill, P. M. W.; Johnson, B. G.; Chen, W.; Wong, M. W.; Andres, J. L.; Head-Gordon, M.; Replogle, E. S.; Pople, J. A. *Gaussian 98*; Gaussian Inc.: Pittsburgh, PA, 1998.
(21) Reed, A. E.; Curtis, L. A.; Weinhold, F. *Chem. Rev.* **1988**, *88*, 849 and references therein.
(22) Flükiger, P.; Lüthi, H. P.; Portann, S.; Weber, J. *MOLEKEL*, v.4.3; Scientific Computing: Manno, Switzerland, 2002−2002. Portman, S.; Lüthi, H. P. *CHIMIA* **2000**, *54*, 766.
(23) Aresta, M.; Nobile, F.; Albano, V. G.; Formni, E.; Manassero, M. *J. Chem. Soc., Chem. Commun.* **1975**, 636.
(24) Bristow, G. S.; Hitchcock, P. B.; Lappert, M. F. *J. Chem. Soc., Chem. Commun.* **1981**, 1145.
(25) Alvarez, R.; Carmona, E.; Marin, J. M.; Poveda, M. L.; Gutierrez-Puebla, E.; Monge, A. *J. Am. Chem. Soc.* **1986**, *108*, 2286.
(26) (a) Sakaki, S. In *Stereochemistry of Organometallic and Inorganic Compounds, Vol. 4, Stereochemical Control, Bonding and Steric Rearrangements*; Bernal, I., Ed.; Elsevier: Amsterdam, 1990; p 95. (b) Sakaki, S.; Kitaura, K.; Morokuma, K. *Inorg. Chem.* **1982**, *21*, 760.

Table 1. Energy Changes[a] by the Interaction of Carbon Dioxide with the Ru Center and the Insertion of Carbon Dioxide into the Ru(II)−H Bond of *cis*-$Ru(H)_2(PMe_3)_3$, the Coordination of Dihydrogen Molecule with $Ru(H)(\eta^1\text{-}OCOH)(PMe_3)_3$ **5**, Isomerization of the η^1-formate Moiety in $Ru(H)(\eta^1\text{-}OCOH)(PMe_3)_3(H_2)$, and the Metathesis of the η^1-Formate Complex with Dihydrogen Molecule

	DFT	MP2	MP3	MP4(DQ)	MP4(SDQ)
Coordination of CO_2 with the Ru Center					
ΔE(**1**→**2**)	−3.2	−17.7	−12.8	−15.2	−16.5
E_a(**2**→**3**)	−0.2	−3.3	−0.9	−1.9	−2.4
ΔE(**2**→**3**)	−7.4	−32.5	−9.7	−20.9	−21.5
Insertion of CO_2 into the Ru(II)−H Bond					
E_a(**3**→**4**)	7.2	26.6	5.9	18.5	17.6
ΔE(**3**→**4**)	4.6	32.4	0.7	18.1	17.9
Isomerization of the η^1-Formate Moiety					
E_a(**4**→**5**)	1.8	5.2	0.3	2.2	3.2
ΔE(**4**→**5**)	1.4	6.1	0.4	2.5	3.8
Coordination of H_2 with the Ru Center of **5**					
ΔE(**5**→**6**)	18.3	31.7	24.1	27.7	28.0
Isomerization of the η^1-Formate Moiety in **6**					
E_a(**6**→**7**)	−2.6	−0.6	−2.7	−1.5	−1.3
ΔE(**6**→**7**)	−5.8	−3.1	−5.9	−2.5	−2.6
Metathesis of the η^1-Formate Complex with Dihydrogen Molecule					
E_a(**7**→**8**)	5.5	7.9	11.3	9.5	9.0
ΔE(**7**→**8**)	5.1	8.4	12.4	8.5	8.7

[a] kcal/mol unit. The BS-II system was used for these calculations.

TS_{3-4} to afford a ruthenium(II) η^1-formate intermediate, $Ru(H)(\eta^1\text{-}OCOH)(PMe_3)_3$ **4**. In **TS_{3-4}**, the H ligand is approaching the C atom of carbon dioxide, and the C−H distance considerably shortens to 1.591 Å. The Ru−H distance moderately lengthens to 1.685 Å, while the OCO angle changes little. In **4**, the C−H bond distance (1.245 Å) of formate is somewhat longer than the usual C−H bond (1.130 Å) of formic acid by about 0.1 Å. These rather long C−H and rather short Ru−H distances suggest that a bonding interaction still exists between the Ru center and the C−H bond like the agostic interaction. Certainly, the 1s orbital of the H atom overlaps well with the unoccupied d_σ orbital of the Ru center, as shown in Figure 2B. The H atomic population is smaller than that of the usual H atom of formate, as will be discussed below. Besides **4**, there is the other isomer of the ruthenium(II) η^1-formate intermediate **5**, which is formed from **4** through the transition state **TS_{4-5}**. In **TS_{4-5}**, the η^1-formate moiety rotates counterclockwise, which weakens the agostic interaction between the C−H bond and the Ru center. The intermediate **5** is coordinatively unsaturated, in which the C−H bond does not interact with the Ru center and the η^1-formate moiety coordinates well with the Ru center; as a result, the Ru−O and C−H distances (2.243 and 1.130 Å, respectively) are considerably shorter than those of **4**.

Energy changes by the insertion reaction were evaluated with the DFT and MP2 to MP4(SDQ) methods, as listed in Table 1. The MP4(SDQ) method presents considerably larger stabilization energy by coordination of carbon dioxide, ΔE(**1**→**2**) and ΔE(**2**→**3**), and considerably larger activation barrier E_a(**3**→**4**) and reaction energy ΔE(**3**→**4**) of the CO_2 insertion than does the DFT method, while these two methods present similar energy changes in the other elementary processes. Although these values somewhat fluctuate around MP2 and MP3 levels of theory, they fluctuate less upon going to MP4(SDQ) from MP3, and the MP4(SDQ) calculated values are intermediate between the MP2 and MP3 calculated values. To examine the reliabilities of DFT and MP4(SDQ) methods, the CCSD(T) method was applied to the insertion of carbon dioxide into the Ru(II)−H bond of the model system, *cis*-$Ru(H)_2(PH_3)_3$, because the real system is too large for us to perform the CCSD(T) calculation. The geometries of the model system were taken to be the same as those of the real system, where three PMe_3 ligands were replaced with three PH_3 ligands. As shown in Table 2, the DFT method presents much smaller reaction energy ΔE(**1**→**3**) and activation barrier Ea(**3**→**4**) than does the CCSD(T) method, while the MP4(SDQ) method presents similar reaction energy ΔE(**1**→**3**) to that of the CCSD(T) method and moderately larger activation barrier E_a(**3**→**4**) than that of the CCSD(T) method. These results suggest that the MP4(SDQ) method seems better than the DFT method in the present catalytic reaction. In this work, we will discuss the results based on both DFT and MP4(SDQ) methods.

Table 2. Comparison of Computational Methods in the Coordination of Carbon Dioxide with the Ru Center and the Insertion of Carbon Dioxide into the Ru(II)−H Bond of Model System, *cis*-$Ru(H)_2(PH_3)_3$

	ΔE(**1**→**3**)[a] (kcal/mol)	E_a(**3**→**4**)[b] (kcal/mol)
DFT	−1.17	5.9
MP2	−36.4	24.5
MP3	−10.6	4.5
MP4(D)	−25.7	17.2
MP4(DQ)	−22.9	16.3
MP4(SDQ)	−25.0	15.7
CCSD	−16.7	8.9
CCSD(T)	−23.4	11.6

[a] ΔE(**1**→**3**) is the stabilization energy of **3** relative to **1**, where a negative value means that **3** is more stable than **1**. [b] E_a represents the energy difference between **3** and **TS_{3-4}**.

The DFT and MP4(SDQ) calculated energy changes with correction of zero-point energy and free energy changes are shown in Figure 3A and B, respectively. Apparently, the activation barrier going to **3** from **2** disappears in both the DFT/BS-II and MP4(SDQ)/BS-II calculations.[27] Thus, the CO_2 complex **2** is not important, and the coordination of carbon dioxide with the Ru center directly affords **3**. The free energy change ($\Delta G_v°$) with only the contribution of vibration movements is −37.1 (−9.0) kcal/mol, which is somewhat smaller than the change in ΔE, where the value without parentheses is the MP4(SDQ) calculated one and that in parentheses is the DFT calculated one, hereafter. The free energy change $\Delta G°$ in gas phase is −28.9 (−0.8) kcal/mol. This value is much smaller than the $\Delta G_v°$ value, because the adduct **3** is formed from **1** and CO_2 in this coordination process. In the CO_2 insertion into the Ru(II)−H bond, the activation barrier is 16.1 (5.6) kcal/mol, and the activation free energy changes are 16.7 (6.2) and 16.7 (6.1) kcal/mol for $\Delta G_v°^{‡}$ and $\Delta G°^{‡}$, respectively. These results clearly indicate that the insertion reaction takes place with moderate activation energy. However, the reverse deinsertion reaction of carbon dioxide more easily takes place with a smaller activation barrier than does the insertion because the insertion is considerably endothermic. This means that the next step must proceed easily to complete the catalytic cycle; if not, the deinsertion of carbon dioxide takes place easily. The next

(27) Although the geometry optimization by the DFT/BS-I method yielded the weak CO_2 complex **2**, the DFT/BS-I calculation indicated that **2** easily converts to **3** with nearly no barrier. The small discrepancy between the DFT/BS-I and DFT/BS-II calculations is not important.

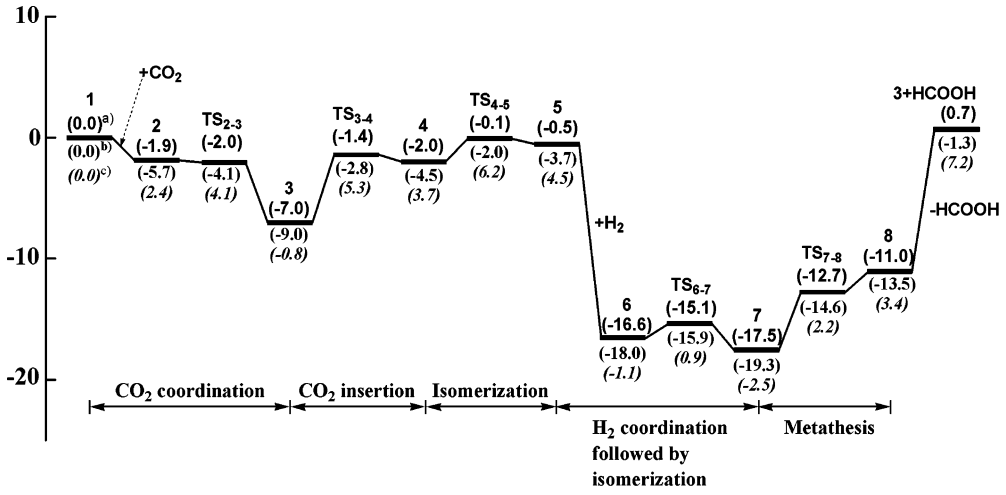

(A) DFT-calculated energy change

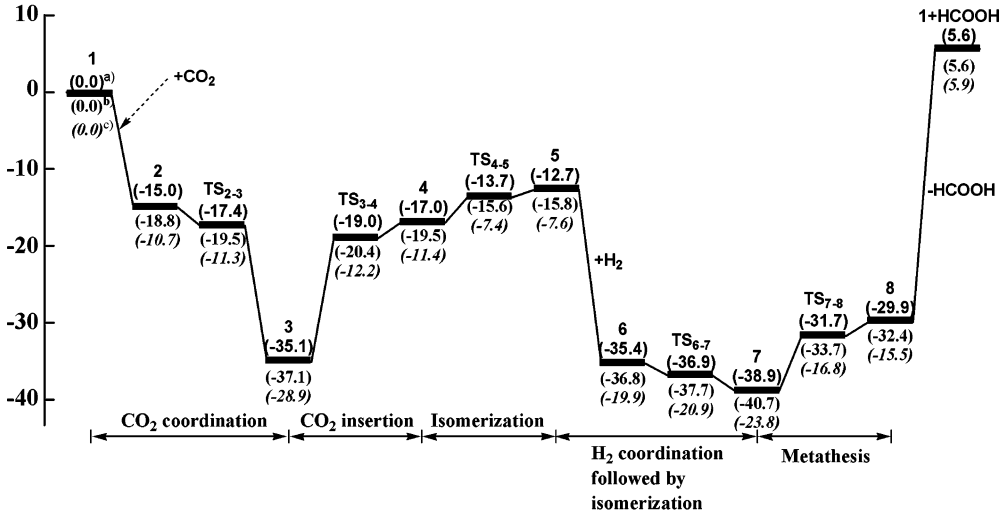

(B) MP4(SDQ)-calculated energy change

Figure 3. Potential energy change (a) and free energy change (b, c) (kcal/mol unit) along the catalytic cycle. (a) Potential energy change with correction of zero-point energy. (b) In the $\Delta G°$ value, contributions of translation, rotation, and vibration movements are considered. (c) In the $\Delta G_v°$ value, contributions of vibration movements are considered, while those of translation and rotation movements are neglected.

step is the isomerization from **4** to **5**. However, this isomerization is endothermic and cannot suppress the deinsertion; note that the intermediate **5** is slightly less stable than **4**. Thus, the coordination of the dihydrogen molecule should occur to suppress the deinsertion of carbon dioxide, as will be discussed below in detail. Although the considerable differences in energy change are observed between the DFT and MP4(SDQ) methods, both methods clearly show that the dihydrogen molecule must coordinate with the Ru center to suppress the deinsertion, as shown in Figure 3.

It should be noted that carbon dioxide is inserted into the Ru(II)−H bond of *cis*-$Ru(H)_2(PMe_3)_3$ with a moderately smaller activation barrier (7.2 kcal/mol) than that (9.5 kcal/mol) of the insertion reaction in *cis*-$Ru(H)_2(PH_3)_3$, where the activation barriers calculated with the DFT method are given without correction of the zero-point energy because the DFT method was used in the previous work.[7] In other words, the donating PMe_3 ligand is more favorable for the insertion of carbon dioxide into the Ru(II)−H bond than the PH_3 ligand. The reason will be discussed below in detail.

Metathesis of the Ruthenium(II)-η^1-formate Intermediate, Ru(H)(η^1-OCOH)$(PMe_3)_3$ 5, with Dihydrogen Molecule: The next step is coordination of the dihydrogen molecule with the Ru center of **5** followed by the metathesis of the ruthenium(II) η^1-formate intermediate with the dihydrogen molecule. Dihydrogen molecule easily coordinates with the Ru center of **5** to afford a ruthenium(II) complex of dihydrogen molecule, Ru(H)(η^1-OCOH)$(PMe_3)_3(H_2)$ **6**, as shown in Figure 4, because **5** possesses an empty coordination site. In **6**, the distances between the Ru center and two H atoms of dihydrogen molecule are 1.738 and 1.710 Å, and the H−H distance (0.879 Å) is considerably longer than the equilibrium distance (0.744 Å by the DFT/BS-I calculation). These geometrical features indicate that the dihydrogen molecule strongly coordinates with the Ru center, as will be shown below by the large stabilization energy.

However, the metathesis cannot take place directly from **6**, because any hydrogen atom of the dihydrogen molecule cannot approach the O atom of formate due to the unfavorable conformation of the formate moiety.[28] Thus, **6** must isomerize to **7** in which one of the oxygen atoms of formate takes a

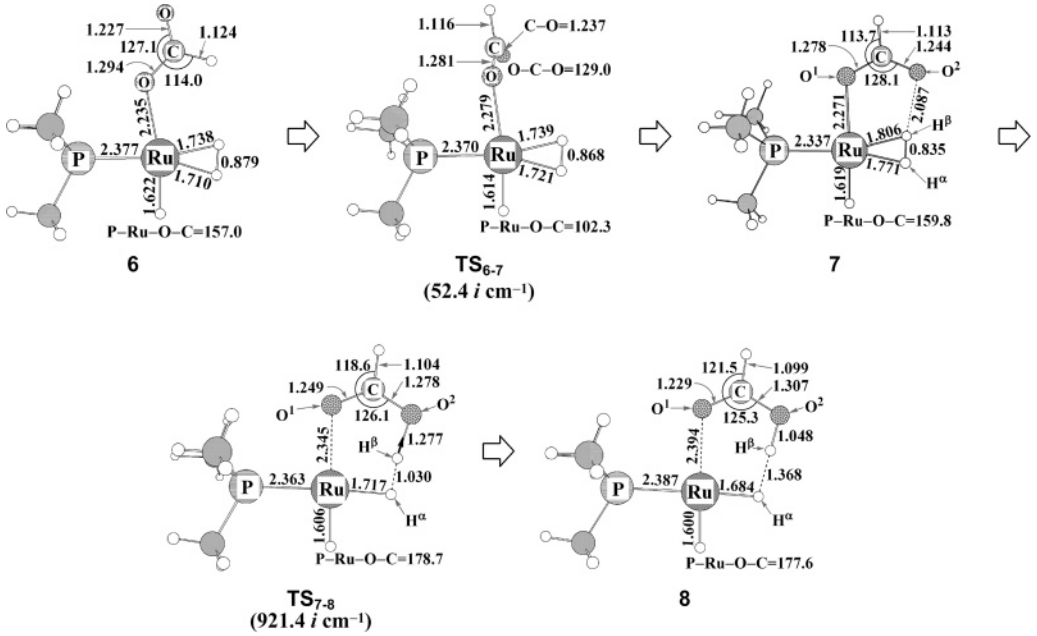

Figure 4. Geometry changes by the isomerization of the ruthenium(II)−formate complex, Ru(H)(η^1-OCOH)(PMe_3)$_3$, and the metathesis of Ru(H)(η^1-OCOH)(PMe_3)$_3$ with the dihydrogen molecule (two PMe_3 ligands in front of and behind the Ru center are omitted in all the figures to show clearly the geometry changes by the reaction). Bond length in angstrom and bond angle in degree. In parentheses is imaginary frequency of the transition state. Arrows in $\mathbf{TS_{6-7}}$ and $\mathbf{TS_{7-8}}$ represent geometry changes involved in each imaginary frequency.

position near to the dihydrogen molecule (see Figure 4). In $\mathbf{TS_{6-7}}$, the formate moiety is almost perpendicular to the O−Ru−(H_2) plane. From **7**, the H−H bond breaking occurs through the transition state $\mathbf{TS_{7-8}}$, to afford a ruthenium(II) complex of formic acid, Ru(H)$_2$(HCOOH)(PMe_3)$_3$ **8**. In $\mathbf{TS_{7-8}}$, the H^β atom is moving from the H^α atom to the O atom of the formate moiety; see Figure 4 for H^α and H^β. The Ru−H^α distance considerably shortens to 1.717 Å, and the position of the H^β atom is almost intermediate between O and H^α atoms. This geometry of $\mathbf{TS_{7-8}}$ is essentially the same as that of the heterolytic C−H σ-bond activation of benzene by the palladium(II)−formate complex.[29] In **8**, the O−H bond distance of formic acid is 1.048 Å, which is considerably longer than the usual O−H bond distance (0.973 Å) of free formic acid. Consistent with this long O−H bond distance, the H^α−H^β distance (1.368 Å) between formic acid and the H^α ligand is rather short, which indicates that some bonding interaction still exists between these two atoms, as will be discussed below. The Ru−O bond distance is 2.394 Å, which is considerably longer than that of **7**. This is interpreted in terms of the change of formate to formic acid, as follows: The formate anion in **7** possesses the C−O^1 single bond and the C=O^2 double bond in a formal sense, because the C−O^1 bond is much longer than the C−O^2 bond. Thus, the O^1 atom, which is more negatively charged than the O^2 atom, coordinates with the Ru center in **7**. In **8**, on the other hand, the C−O^1 bond becomes a double bond and the C−O^2 bond becomes a single bond because the H atom is bound with the O^2 atom. In other words, the O^1 atom possesses −1 formal charge in **7**, but it is neutral in **8** in a formal sense. As a result, the η^1-formate ligand much more strongly coordinates with the Ru center in **7** than does formic acid in **8**, which leads to the longer Ru−O^1 distance in **8** than in **7**.

Now, we wish to discuss the energy changes along these processes. As suggested from the geometry of **6**, the coordination of the dihydrogen molecule induces considerably large stabilization energy. Although significantly large differences between the DFT and MP4(SDQ) methods are not observed in energy changes of metathesis, the DFT method underestimates the stabilization energy by the coordination of the dihydrogen molecule with the Ru center, compared with the MP4(SDQ) method, as listed in Table 1. The stabilization energy converges to ca. 28 kcal/mol upon going to MP4(SDQ) from MP3. Considering these results and the stabilization energy by the coordination of carbon dioxide with **1** (see above), the MP4(SDQ) method seems better than the DFT method in evaluating the stabilization energy by the coordination of dihydrogen molecule. However, both DFT and MP4(SDQ) methods lead to the same conclusion about the reaction mechanism, as will be shown below.

As shown in Figure 3, **5** undergoes the coordination of dihydrogen molecule with significantly large free energy decrease; the free energy change ($\Delta G_v°$) with only the contribution of vibration movements is −21.0 (−14.3) kcal/mol, and the usual free energy change ($\Delta G°$) is −12.3 (−5.6) kcal/mol. It should be noted that the $\Delta G°$ value is considerably negative even in the gas phase. As discussed above, the stabilization of **5** is necessary to suppress the deinsertion of carbon dioxide, because the deinsertion more easily occurs with a smaller activation barrier than does the insertion (vide supra). If the concentration of dihydrogen molecule was not sufficiently large, **5** could not easily undergo the coordination of the dihydrogen molecule, and as a result, the deinsertion took place. Therefore,

(28) From **6**, the metathesis with the dihydrogen molecule can take place through the four-center transition state. However, our previous theoretical study indicated that the six-center transition state is much lower in energy than the four-center transition state in the metathesis of the ruthenium(II)-η^1-formate complex with the dihydrogen molecule.[7] Thus, it is likely to consider that the metathesis takes place through the six-center transition state if the isomerization of **6** easily takes place with a moderate activation barrier.

(29) Biswas, B.; Sugimoto, M.; Sakaki, S. *Organometallics* **2000**, *19*, 3895.

Scheme 2

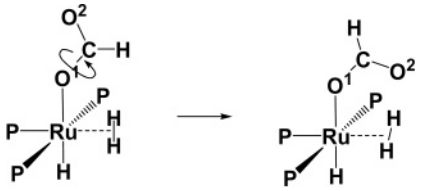

(A) Isomerization of Ru(H)(η^1-OCOH)(PMe_3)$_3$(H_2)

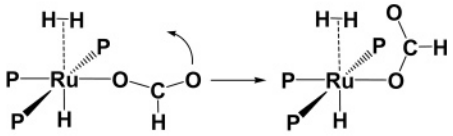

(B) Isomerization of Ru(H)(η^1-OCOH)(PH_3)$_3$(H_2)

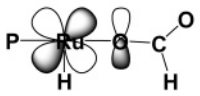

(C) Exchange repulsion between d_π orbital of Ru and lone pair orbital ofη^1-formate

the catalytic reaction is suppressed when the dihydrogen molecule is not sufficiently supplied. This means that the reaction rate depends on the pressure of the dihydrogen molecule, as reported experimentally.[6b,c]

The next step is the isomerization of the ruthenium(II)-η^1-formate intermediate from **6** to **7**. The DFT/BS-II and MP2 to MP4(SDQ)/BS-II methods present a negative activation barrier, probably because of some artificial error. However, it is reasonably concluded that this isomerization easily occurs with nearly no barrier. The nearly no activation barrier is not surprising because this isomerization takes place through the rotation of the formate moiety about the C−O^1 bond, as shown in Scheme 2A. Finally, the H−H bond breaking takes place with the E_a value of 7.2 (4.7) kcal/mol and the $\Delta G^{\circ\ddagger}$ and $\Delta G_v^{\circ\ddagger}$ values of 7.0 (4.7) kcal/mol. Because these E_a and $\Delta G^{\circ\ddagger}$ values are smaller than those of the insertion reaction in both DFT and MP4(SDQ) calculations, it should be concluded that the insertion of carbon dioxide into the Ru(II)−H bond is the rate-determining step.

Energy Changes along Whole Catalytic Cycle and Solvent Effects: Here, we wish to summarize the energy changes along the catalytic cycle. Apparently, the MP4(SDQ) method provides the substantially larger stabilization energy by the coordination of carbon dioxide (**1** → **3**) and dihydrogen molecule (**5** → **6**) and the substantially larger activation barrier and endothermicity of the CO_2 insertion (**3** → **5**) than does the DFT method, while the energy changes in the other elementary steps are not different very much. Despite the above-mentioned differences, both methods show common features in energy changes; (1) the coordination of carbon dioxide with the Ru center is exothermic, (2) the insertion of carbon dioxide into the Ru(II)−H bond followed by the isomerization of the η^1-formate is endothermic, (3) the rate-determining step is the insertion of carbon dioxide into the Ru(II)−H bond, and (4) the coordination of dihydrogen molecule is considerably exothermic enough to suppress the deinsertion.

Solvent effects were evaluated with the DPCM method,[12] where *n*-heptane was selected because super critical carbon dioxide is considered to be similar to normal alkane. Also, solvent effects by THF were investigated to present some information about the use of polar solvent. Interestingly, the activation barrier of the metathesis considerably increases in the order gas phase < *n*-heptane < THF, as shown in Table 3, while the activation barrier and the reaction energy of the CO_2 insertion moderately decrease in the order gas phase > *n*-heptane > THF.[30]

Table 3. Solvation Effects on the Free Energy Changes[a] of Important Elementary Steps

	gas phase		*n*-heptane		THF	
	$\Delta G_v^{\circ\ddagger}$	ΔG_v°	$\Delta G_v^{\circ\ddagger}$	ΔG_v°	$\Delta G_v^{\circ\ddagger}$	ΔG_v°
CO_2 Coordination						
2 → **3**	1.6	−3.3	−1.8	−9.8	1.5	−10.7
CO_2 Insertion						
3 → **4**	6.2	4.5	5.4	3.4	5.3	2.5
Isomerization of Formate in Ru(H)(η^1-OCOH)(PMe_3)$_2$						
4 → **5**	2.5	0.8	1.0	0.7	0.4	0.2
Coordination of Dihydrogen Molecule						
5 → **6**		−14.3		−12.0		−16.4
Isomerization of Formate in Ru(H)(η^1-OCOH)(PMe_3)$_2$(H_2)						
6 → **7**	2.1	−1.3	−1.9	−4.9	0.2	−3.3
Metathesis with Heterolytic H−H Bond Activation						
7 → **8**	4.7	5.8	6.3	8.5	7.4	10.0

[a] ΔG_v° values (in kcal/mol) are provided here. The DFT/BS-II method was employed to evaluate the electronic energy.

It is worthy of investigation to clarify the reason that the metathesis (**7**→**8**) becomes difficult in polar solvent. This is easily interpreted in terms that **7** consists of the anionic formate and the positively charged Ru moieties but **8** consists of neutral formic acid and the neutral Ru moieties in a formal sense; in other words, the highly polar species converts to the less polar species in the metathesis. Thus, the polar solvent is not favorable for the metathesis. It is also interesting that the activation barrier of the CO_2 insertion into the Ru(II)−H bond moderately decreases in the order gas phase > *n*-heptane > THF, while

(30) The energy changes by the DFT method indicate that the rate-determining step becomes the metathesis in *n*-heptane and THF, while those by the MP4(SDQ) method indicate that the rate-determining step is the CO_2 insertion in *n*-heptane and THF.

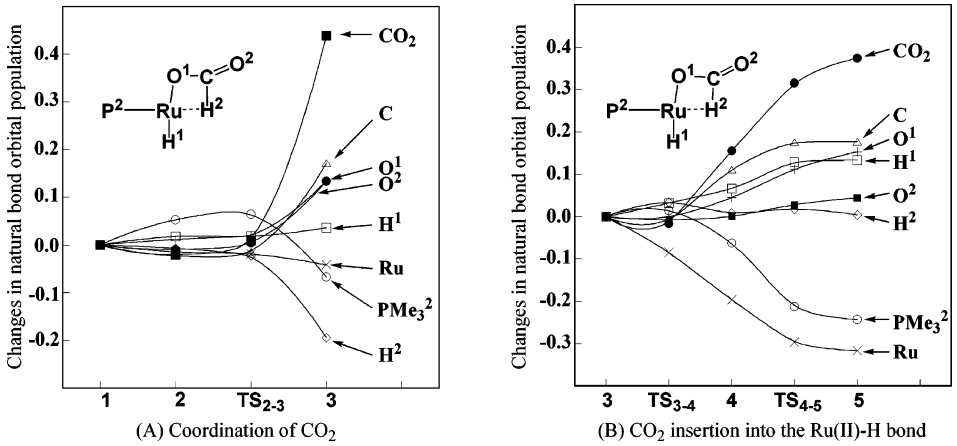

Figure 5. Population changes in the coordination of carbon dioxide with the Ru center and the insertion reaction of carbon dioxide into the Ru(II)−H bond. NBO populations are shown here. The positive value represents the increase in electron population, and vice versa.

Scheme 3

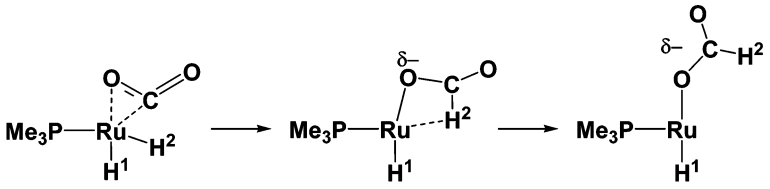

	3	TS_{3-4}	4	TS_{4-5}	5
Dipole moment	6.47 D	6.27 D	7.52 D	8.24 D	8.10 D
Natural charge	$H^1 = 0.004$ $H^2 = 0.023$ $CO_2 + H^2 = -0.417$		$H^1 = -0.062$ $H^2 = 0.014$ $OCOH^2 = -0.588$		$H^1 = -0.128$ $H^2 = 0.019$ $OCOH^2 = -0.794$

the reaction energies ΔE(**3**→**4**) and ΔE(**4**→**5**) decrease in the order gas phase > *n*-heptane > THF to a greater extent than does E_a(**3**→**4**). This is interpreted in terms that the transition state $\mathbf{TS_{3-4}}$ is similar to the intermediate **3**; actually, the dipole moments of **3** and $\mathbf{TS_{3-4}}$ are 6.47 and 6.27 D, as shown in Scheme 3. In other words, the ruthenium(II) η^2-carbon dioxide complex **3** contains the considerably strong CT interaction between the π^* orbital of CO_2 and the d_π orbital of Ru, the strength of which is similar to that of the polarized $\mathbf{TS_{3-4}}$.[31] Upon going to **4** from $\mathbf{TS_{3-4}}$, the dipole moment considerably increases, because the charge transfer becomes considerably strong in **4**. As a result, polar solvent such as THF decreases the reaction energy ΔE(**3**→**4**) to a greater extent than E_a(**3**→**4**) (see Table 3). Upon going to **5** from **4**, the dipole moment further increases, and therefore, polar solvent decreases E_a(**4**→**5**) and ΔE(**4**→**5**). This is because the anionic η^1-formate takes a position more distant from the positively charged Ru center in **5** than in **4**. Considering these solvent effects, the polar solvent facilitates the CO_2 insertion reaction.

Population Changes and Electronic Process in the Insertion Reaction and Their Differences between the PMe_3 Complex and the PH_3 Analogue: Although significant differences in reaction behavior between PMe_3 and PH_3 have not been reported in the transition-metal complexes of dihydrogen molecule[32] and the oxidative addition of dihydrogen molecule to $Pt(PR_3)_2$,[33] it is worthwhile to discuss here the differences in the CO_2 insertion reaction between the PMe_3 and PH_3 complexes. The differences are summarized as follows. (1) The ruthenium(II) complex of carbon dioxide **3** exists as an intermediate in the PMe_3 system, while it did not exist in the PH_3 system.[7] (2) The η^1-OCOH moiety takes a position trans to PH_3 in $Ru(H)(\eta^1\text{-}OCOH)(PH_3)_3$, while it is at a position trans to the H(hydride) ligand in $Ru(H)(\eta^1\text{-}OCOH)(PMe_3)_3$. And, (3) the insertion reaction takes place with the moderately smaller activation barrier in the PMe_3 system than in the PH_3 system.

Electron populations are useful to find reasons of these differences. The electron population of carbon dioxide considerably increases upon going to **3** from **1**, as shown in Figure 5A. The increase in electron population of carbon dioxide is in general observed in the coordination of carbon dioxide with the transition-metal complex, because the charge transfer from the metal center to carbon dioxide mainly contributes to the coordinate bond of carbon dioxide with the metal center.[26] In **3**, the π^* orbital of carbon dioxide overlaps well with the d_π orbital of the Ru center, as discussed above and in Figure 2A. This π-back-donation is stronger in *cis*-$Ru(H)_2(PMe_3)_3(CO_2)$ than in the PH_3 analogue, because PMe_3 is more donating than PH_3, as shown by their lone pair orbital energies; the lone pair orbital of PMe_3 is at −8.91 (−6.00) eV and that of PH_3 is at −10.54 (−7.57) eV, where the values without parentheses are Hartree−Fock orbital energies and in parentheses are Kohn−Sham orbital energies. As a result, *cis*-$Ru(H)_2(PMe_3)_3(CO_2)$

(31) Electron populations little change upon going from **3** to $\mathbf{TS_{3-4}}$, as shown in Figure 5. Thus, no factor that slightly decreases the dipole moment in $\mathbf{TS_{3-4}}$ is found in electron population changes.

(32) Eckert, J.; Kubas, G. J.; Hall, J. H.; Hay, J.; Boyle, C. M. *J. Am. Chem. Soc.* **1990**, *112*, 2324.

(33) Matsubara, T.; Maseras, F.; Koga, N.; Morokuma, K. *J. Phys. Chem.* **1996**, *100*, 2503.

exists as a stable intermediate but the PH_3 analogue does not. However, the Ru atomic population decreases little in **3**, unexpectedly, while the electron populations of the H and PMe_3[2] ligands decrease in **3**. Because the C−H distance is very long, the direct interaction between the H ligand and carbon dioxide is not formed. It is likely to consider that the charge transfer from the Ru center to carbon dioxide occurs and the Ru center is supplied the electron density by the H and PMe_3[2] ligands.

In the insertion reaction, the electron population of carbon dioxide further increases, while the electron populations of the Ru center and PMe_3[2] decrease, as shown in Figure 5B. These population changes clearly show that the charge-transfer from $Ru(H)_2(PMe_3)_3$ to carbon dioxide significantly occurs in the insertion reaction, as reported previously.[34] Because PMe_3 possesses its lone pair orbital at a higher energy than that of PH_3 (see above), the PMe_3 complex is more favorable for this charge-transfer than the PH_3 complex, as follows: (1) The H^2 atomic population is 1.172e in *cis*-$Ru(H)_2(PMe_3)_3$ and 1.115e in *cis*-$Ru(H)_2(PMe_3)_3$. (2) The molecular orbital $\varphi(H_{1s})$, which mainly consists of the 1s orbital of the H ligand, participates in the charge transfer to carbon dioxide. This $\varphi(H_{1s})$ orbital is at −8.61 (−5.82) eV in *cis*-$Ru(H)_2(PMe_3)_3$ but at −9.44 (−6.76) eV in *cis*-$Ru(H)_2(PH_3)_3$, where the values without parentheses are Hartree−Fock orbital energies (HF/BS-II) and those in parentheses are Kohn−Sham orbital energies (DFT/BS-II). And, (3) the Ru(II)−H bond is weaker in *cis*-$Ru(H)_2(PMe_3)_3$ than in *cis*-$Ru(H)_2(PH_3)_3$, because of the stronger trans influence of PMe_3 than that of PH_3; actually, the Ru(II)−H bond (1.661Å) is considerably longer in *cis*-$Ru(H)_2(PMe_3)_3$ than that (1.641Å) in *cis*-$Ru(H)_2(PH_3)_3$. From all these factors, carbon dioxide is more easily inserted into the Ru(II)−H bond in *cis*-$Ru(H)_2(PMe_3)_3$ than in *cis*-$Ru(H)_2(PH_3)_3$. We wish to mention here that the H^2 atomic population changes little upon going to **4** from **3**, unexpectedly, despite the charge transfer from $Ru(H)_2(PMe_3)_3$ to carbon dioxide. This result is interpreted in terms that the H^2 ligand is supplied electron density by the Ru center and PMe_3[2].

The difference in geometry between Ru(H)(η^1-OCOH)$(PMe_3)_3$ and the PH_3 analogue is also understood in terms of the trans influence of PMe_3 and PH_3. Because the H ligand exhibits much stronger trans influence than PH_3, the η^1-OCOH moiety tends to avoid the position trans to the H ligand. As a result, the η^1-OCOH moiety takes a position trans to PH_3 in Ru(H)(η^1-OCOH)$(PH_3)_3$ $\mathbf{5_Hb}$ (see Figure 6A). This structure is considerably more stable than the other one $\mathbf{5_H}$ by 18.4 kcal/mol in which the η^1-OCOH moiety is at a position trans to the H ligand (Figure 6A). Because $\mathbf{5_H}$ is much less stable than $\mathbf{5_Hb}$, not $\mathbf{5_H}$ but $\mathbf{5_Hb}$ is easily formed by the insertion reaction in the PH_3 system unlike that in the PMe_3 system, as reported previously.[7] On the other hand, Ru(H)(η^1-OCOH)$(PMe_3)_3$ **5** is moderately less stable than the other structure **5b**, where the η^1-OCOH moiety is at a position trans to the H(hydride) ligand in **5** and at a position trans to PMe_3 in **5b** (see Figure 6B). This is because PMe_3 exhibits a much stronger trans influence than PH_3, and the trans influence is not very much different between hydride and PMe_3 ligands. As a result, the insertion reaction of carbon dioxide yields **5**; note that the position change of carbon dioxide must necessarily occur to afford **5b**, which needs an additional activation barrier because carbon dioxide must move across the doubly occupied d_π orbital of Ru to afford **5b**. Moreover, the intermediate **5b** does not easily undergo the metathesis with the dihydrogen molecule, as will be discussed below, whereas **5b** is slightly more stable than **5**. Thus, **5b** is not important in the catalytic cycle.

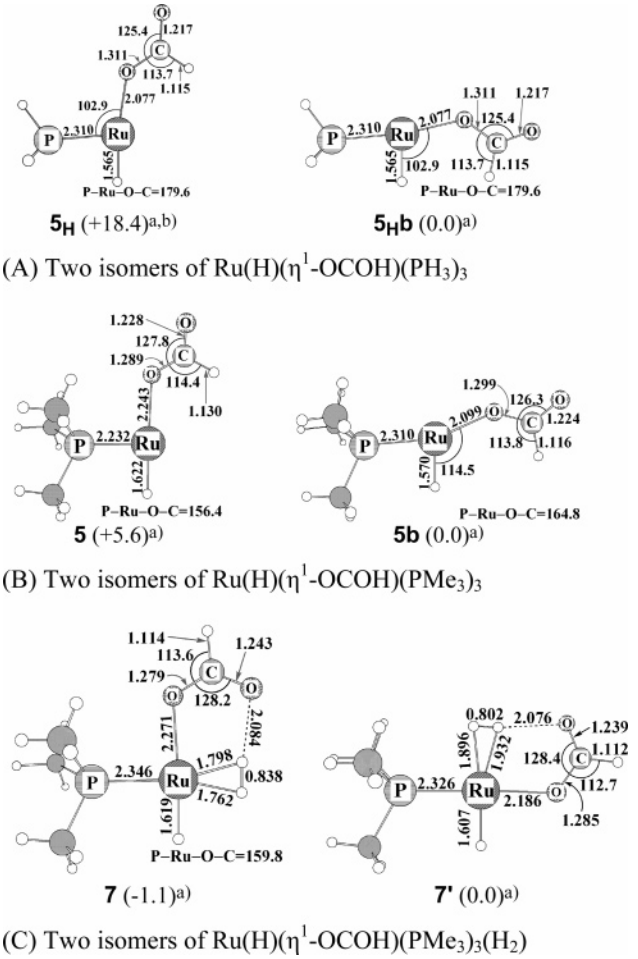

Figure 6. Geometries of two isomers of Ru(H)(η^1-OCOH)$(PH_3)_3$, Ru(H)(η^1-OCOH)$(PMe_3)_3$, and Ru(H)(η^1-OCOH)$(PH_3)_3(H_2)$. Bond length in angstrom and bond angle in degree. (a) In parentheses are the relative energy (in kcal/mol) calculated with the DFT/BS-II method. (b) $\mathbf{5_H}$ converts to $\mathbf{5_Hb}$ during the geometry optimization. $\mathbf{5_H}$ is an assumed structure in which the P−Ru−O angle was taken to be 90.0°. (c) Two PMe_3 ligands in front of and behind the Ru center are omitted in all the figures to show clearly the geometry changes by the reaction.

At the end of this section, we wish to discuss the bonding interaction between formate and the Ru center in **4** which was mentioned above. The H atomic population of free formate is 1.105e but decreases to 0.986e in **4** (see Supporting Information Figure S1). This small H atomic population in **4** indicates that the 1s orbital of the H atom interacts with the unoccupied d_σ orbital of the Ru center.

Population Changes by Coordination of Dihydrogen Molecule with the Ru Center and Their Differences between PMe_3 and PH_3 Systems: Although the ruthenium(II) η^1-formate intermediate **5** possesses an empty coordination site at a position trans to PMe_3, the PH_3 analogue possesses such an empty coordination site at a position trans to the H ligand. Thus, the ruthenium complex of the dihydrogen molecule takes a different

(34) (a) Sakaki, S.; Ohkubo, Y. *Inorg. Chem.* **1989**, *28*, 2583. (b) Sakaki, S.; Ohkubo, Y. *Inorg. Chem.* **1987**, *27*, 2020. (c) Sakaki, S.; Ohkubo, Y. *Organometallics* **1989**, *8*, 2970. (d) Sakaki, S.; Musashi, Y. *J. Chem. Soc., Dalton Trans.* **1994**, 3047. (e) Sakaki, S.; Musashi, Y. *Inorg. Chem.* **1995**, *34*, 1914. (f) Sakaki, S.; Musashi, Y. *Int. J. Quant. Chem.* **1996**, *57*, 481. (g) Musashi, Y.; Sakaki, S. *J. Chem. Soc., Dalton Trans.* **1998**, 577.

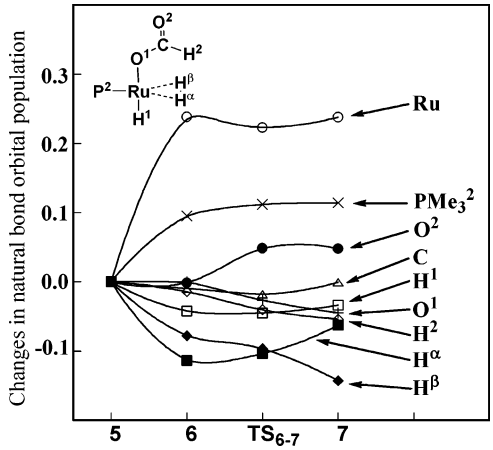

Figure 7. Population changes by the coordination of dihydrogen molecule with the Ru center followed by the isomerization of the ruthenium(II)- η^1-formate complex Ru(H)(η^1-OCOH)(PMe_3)$_3$. The positive value represents the increase in electron population, and vice versa.

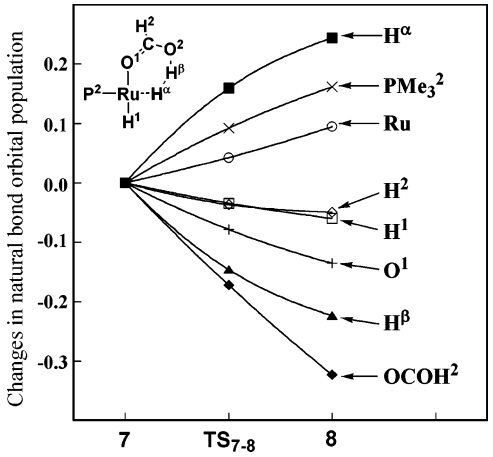

Figure 8. Population changes by the metathesis of the ruthenium(II)-formate complex, Ru(H)(η^1-OCOH)(PMe_3)$_3$, with dihydrogen molecule. The positive value represents the increase in electron population, and vice versa.

geometry between PMe_3 and PH_3 systems; in the PMe_3 system, the dihydrogen molecule is at a position trans to PMe_3, while it is at a position trans to the H ligand in the PH_3 system. As a result, the new H ligand is formed at a position trans to PMe_3 in the PMe_3 system, while it is formed at a position trans to the H ligand in the PH_3 system. The difference in geometry of the ruthenium(II) η^1-formate intermediate leads to differences in the coordination of the dihydrogen molecule and the metathesis between PMe_3 and PH_3 systems, as will be discussed below.

As shown in Figure 7, the electron population of dihydrogen molecule decreases and those of Ru and PMe_3^2 increase in the coordination of the dihydrogen molecule with the Ru center, where PMe_3^2 is at a position trans to the dihydrogen molecule. These results indicate that dihydrogen molecule induces the charge transfer from the dihydrogen molecule to the Ru center, to suppress the charge transfer from PMe_3^2 to the Ru center. The stabilization energy by the coordination of dihydrogen molecule is 16.1 kcal/mol in the PMe_3 system, which is much larger than that (7.6 kcal/mol) of the PH_3 system, where these energies were evaluated with the DFT/BS-II method and the zero-point energy was not added. This is because the dihydrogen molecule takes a position trans to the H ligand in the PH_3 system but at a position trans to PMe_3 in the PMe_3 system. Because the deinsertion is suppressed by coordination of dihydrogen molecule with the Ru center, the PMe_3 system is more favorable for the suppression of the deinsertion than the PH_3 system. This means that the PMe_3 system is better than the PH_3 system for this catalytic reaction.

Population Changes and Electronic Process in the Isomerization of the Ruthenium(II) η^1-Formate Intermediate Followed by the Metathesis with Dihydrogen Molecule, and Their Differences between the PMe_3 Complex and the PH_3 Analogue: Interesting differences between the PMe_3 and PH_3 systems are observed in the isomerization of the ruthenium(II) η^1-formate intermediate and the metathesis with the dihydrogen molecule, as follows: (1) The isomerization of the ruthenium(II) η^1-formate more easily occurs in the PMe_3 system than in the PH_3 system. (2) The geometry changes in the metathesis are different between these two systems. And, (3) the metathesis takes place with a smaller activation barrier in the PMe_3 system than in the PH_3 system.

As mentioned above, the isomerization of the ruthenium(II) η^1-formate intermediate occurs with a considerably large activation barrier (8.5 kcal/mol) in the PH_3 system but with nearly no barrier (−2.6 kcal/mol) in the PMe_3 system, where the activation barrier in parentheses are calculated with the DFT/BS-II method. This is because the isomerization occurs in a different manner between PMe_3 and PH_3 systems. In the PMe_3 system, the isomerization of **6** occurs via the rotation of the formate moiety about the C−O^1 bond (Scheme 2A). Such isomerization does not need a large activation barrier, because the Ru-η^1-OCOH bond is little weakened by the rotation. On the other hand, the isomerization of the PH_3 system occurs in a different way, as shown in Scheme 2B. In the transition state, the lone pair orbital of the η^1-formate anion deviates from the direction toward the Ru center. Thus, this geometry gives rise to the Ru−O bond weakening and the exchange repulsion between the doubly occupied d_π orbital of Ru and the lone pair orbital of formate, as shown in Scheme 2C. As a result, the activation barrier of the isomerization becomes large in the PH_3 system.

In the metathesis, the H^β atomic population considerably decreases, while the H^α atomic population considerably increases, as shown in Figure 8. These population changes clearly show that the metathesis occurs via the heterolytic H−H bond breaking in which the H^β atom becomes a proton and the H^α atom becomes a hydride. Also, the O^1 atomic population considerably decreases, because the formate anion changes into formic acid and the O^1 atom becomes neutral in formic acid in a formal sense. The electron population of Ru increases upon going to **8** from **7**, probably because the H^α (hydride) ligand, which is formed at a position trans to PMe_3, supplies electron density to the Ru center. This H^α ligand suppresses the electron donation of PMe_3 to the Ru center, which leads to an increase in the electron population of PMe_3. In **8**, the H^α and H^β atomic populations are 1.182e and 0.534e, respectively. This result indicates that the electrostatic stabilization interaction exists between the positively charged H^β atom and the negatively charged H^α atom. The H^β atomic population is somewhat larger than that of free formic acid. This electron population suggests that the charge transfer occurs from the H^α ligand to the LUMO of formic acid in **8**; actually, the LUMO of formic acid mainly

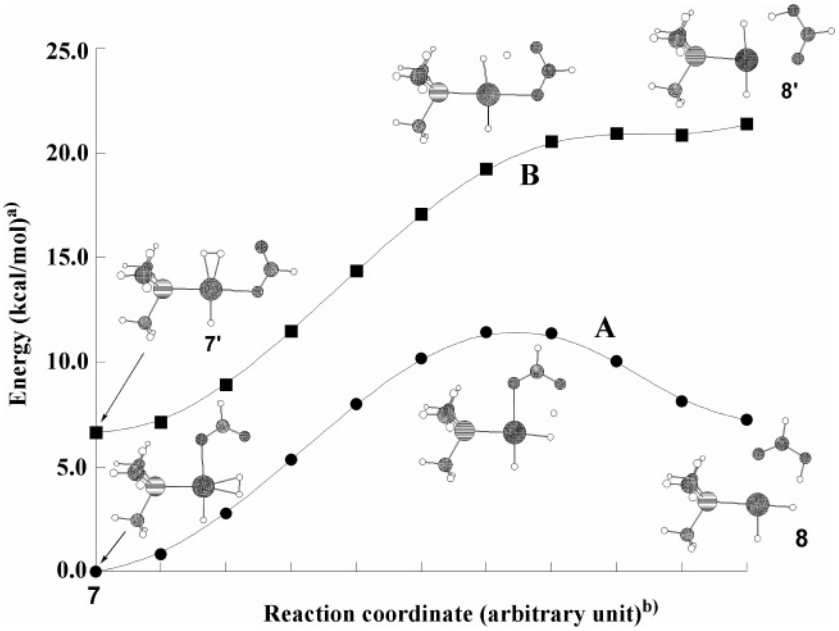

Figure 9. Potential energy changes by the IRC calculation of metathesis starting from **7** to **8** and the assumed geometry changes of the metathesis starting from **7′** to **8′**. (a) The DFT/BS-II calculation (in kcal/mol). (b) Reaction coordinate from IRC calculation. See Figure 6 for **7** and **7′**. In the reaction from **7′** to **8**, the position of H_2 and η^1-formate moiety are exchanged to each other in the IRC calculation of the metathesis from **7** to **8**. Two PMe_3 ligands in front of and behind the Ru center are omitted in all the figures to show clearly the geometry changes by the reaction.

consists of the 1s orbital of H^{β} and extends toward H^{α} (see Supporting Information Figure S3).

The metathesis of Ru(H)(η^1-OCOH)(PMe_3)$_3$ **7** with dihydrogen molecule occurs with a smaller activation barrier in the PMe_3 system than that (E_a = 8.2 kcal/mol) in the PH_3 system. This is interpreted in terms of the trans influence of the H and PMe_3 ligands, as follows: In the metathesis of the PH_3 system, the H(hydride) ligand is formed at a position trans to the H(hydride) ligand. This structure is unfavorable because two hydride ligands are at positions trans to each other; remember that the hydride ligand exhibits strong trans influence. In the metathesis of the PMe_3 system, on the other hand, it is formed at a position trans to PMe_3. Thus, the metathesis of the PMe_3 system more easily occurs than that of the PH_3 system.

It should be investigated here whether the metathesis takes place in the PMe_3 system when it starts from **5b**, because **5b** is moderately more stable than **5** and the metathesis takes place from the similar intermediate $\mathbf{5_Hb}$ in the PH_3 system (see Figure 6 for **5**, **5b**, $\mathbf{5_H}$, and $\mathbf{5_Hb}$). First, two isomers (**7** and **7′**) of Ru(H)(η^1-OCOH)(PMe_3)$_3$(H_2) were optimized, as shown in Figure 6C, where the dihydrogen molecule is at a position trans to PMe_3 in **7** but at a position trans to the H ligand in **7′** (see Figures 6 and 9 for **7** and **7′**). These two isomers are in similar energy to each other (see Figure 9). Then, we tried to optimize *trans*-Ru(H)(PMe_3)$_2$(HCOOH) **8′**, in which formic acid is at a position trans to PMe_3. This is the product of metathesis starting from **7′**. However, **8′** returns to **7′** during the geometry optimization of **8′**. Thus, we performed IRC calculation of the metathesis starting from **7** to **8**, as shown in Figure 9 (line A), and then calculated the energy changes along the geometry changes in which the positions of H_2 and η^1-OCOH are exchanged with each other, as shown in Figure 9 (line B). The latter geometry changes are considered the reasonable model of the metathesis starting from **7′** to **8′**. Apparently, the metathesis starting from **7′** is considerably endothermic (see the line B of Figure 9). More important is that the reverse reaction (**8′**→**7′**) occurs with nearly no barrier. On the other hand, the metathesis easily proceeds from **7** to **8** with a moderate activation barrier (see line A of Figure 9). These results clearly indicate that the metathesis can occur only when the dihydrogen molecule is at a position trans to PMe_3. In the PH_3 system, on the other hand, the metathesis can take place even when the dihydrogen molecule is at a position trans to the H ligand like **7′**, as reported previously.[7] This difference between PMe_3 and PH_3 systems is interpreted as follows: Because the lone pair orbital of PMe_3 is at higher energy than that of PH_3, PMe_3 pushes up the d_σ orbital of Ru in energy to a greater extent than does PH_3. As a result, the $d_\sigma-p_\sigma$ mixing takes place in the PMe_3 system to a greater extent than in the PH_3 system. This $d_\sigma-p_\sigma$ mixing strengthens one Ru−H bond but weakens the other Ru−H bond, as shown in Scheme 4. Consequently, one H ligand tends to dissociate from the Ru center in **8′** to form dihydrogen molecule; in other words, **8′** easily returns to **7′**. In the PH_3 system, such $d_\sigma-p_\sigma$ mixing does not take place effectively because the d_σ orbital of Ru is at considerably low energy in the PH_3 system. Thus, **8′** is not stable, and the metathesis cannot take place from **7′** to **8′** in the PMe_3 system unlike the metathesis in the PH_3 system.

Scheme 4

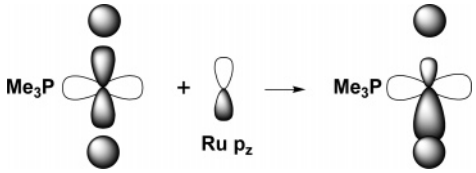

From these results, it is concluded that **5b** and **7′** are not important in the catalytic cycle of the PMe_3 system but **5** is an important intermediate which undergoes easily the coordination of the dihydrogen molecule to afford **6** and that the isomerization of the η^1-formate moiety followed by the metathesis easily takes place starting from **6** through **7** in the PMe_3 system.

Conclusions

Reaction mechanism of hydrogenation of carbon dioxide to formic acid catalyzed by *cis*-$Ru(H)_2(PMe_3)_3$ was theoretically investigated with the DFT and MP4(SDQ) methods. This reaction takes place through the insertion of carbon dioxide into the Ru(II)−H bond, the coordination of the dihydrogen molecule to the ruthenium(II) η^1-formate intermediate, the isomerization of the ruthenium(II) η^1-formate intermediate, and the metathesis of the ruthenium(II) η^1-formate intermediate with the dihydrogen molecule. The rate-determining step is the insertion of carbon dioxide into the Ru(II)−H bond. Although this is not consistent with the experimental results seemingly, the coordination of dihydrogen molecule with the ruthenium(II) η^1-formate intermediate **5** necessarily takes place after the insertion reaction, to suppress the deinsertion. Thus, the reaction rate increases with an increase in the pressure of the dihydrogen molecule, which is consistent with the experimental results.

In the PMe_3 system, the ruthenium(II) η^2-carbon dioxide complex exists as an intermediate, unlike the PH_3 system. Also, the ruthenium(II) η^1-formate intermediate takes a different geometry between PMe_3 and PH_3 systems; in the former system, the η^1-formate takes a position trans to the H ligand, while it takes a position trans to PH_3 in the latter one. The insertion of carbon dioxide into the Ru(II)−H bond occurs with a somewhat smaller activation barrier in the PMe_3 system than that in the PH_3 system. These results are clearly interpreted in terms of the much stronger donation ability and trans influence of PMe_3 than those of PH_3.

The isomerization of the ruthenium(II) η^1-formate intermediate takes place with a much smaller activation barrier in the PMe_3 system than in the PH_3 system. This is because the η^1-formate intermediate of the PMe_3 system takes a different geometry from that of the PH_3 system due to the stronger trans influence of PMe_3 than that of PH_3. Also, the metathesis more easily proceeds in the PMe_3 system than in the PH_3 system, because of the different geometries of the ruthenium(II) η^1-formate intermediate. Thus, it is concluded that the use of a donating ligand is recommended for this catalytic reaction because the donating ligand facilitates the insertion of carbon dioxide into the Ru(II)−H bond, the coordination of dihydrogen molecule with the Ru center, the isomerization of the ruthenium(II) η^1-formate intermediate, and the metathesis.

Solvent effects were also investigated with the DPCM method. Interestingly, a nonpolar solvent facilitates the metathesis, while a polar solvent facilitates the insertion of carbon dioxide into the Ru(II)−H bond. Thus, the use of polar solvent is recommended for this catalytic reaction because the insertion reaction is the rate-determining step.

In conclusion, the experimental results are reasonably interpreted theoretically, and the conclusive discussion of the reaction mechanism and each elementary step are presented here. We wish to present the prediction that the strongly donating ligand and the polar solvent would improve the efficiency of this catalytic reaction. Of course, the present study does not explain all the experimental results of ruthenium-catalyzed hydrogenation of carbon dioxide; for instance, interesting experimental results of the effects of bidentate phosphine ligand[35] and the acceleration by water and alcohol[6b,c,36] have not been theoretically investigated here. In particular, the effects of additives such as water and alcohol are of considerable importance, because of the possibilities that these additives lower the activation barrier of the conversion of carbon dioxide to formate, as experimentally[37] and theoretically suggested.[38] These issues should be theoretically investigated in near future.

Acknowledgment. This work was financially supported by Grants-in-Aid on basic research (No. 15350012), Priority Areas for "Reaction Control of Dynamic Complexes" (No.420), NAREGI project, and Creative Scientific Research from the Ministry of Education, Science, Sports, and Culture. Some of the theoretical calculations were performed with SGI workstations from the Institute for Molecular Science (Okazaki, Japan), and some of them were carried out with PC cluster computers from our laboratory.

Supporting Information Available: Cartesian coordinates of important species including transition states. Electron distribution in $Ru(H)(\eta^1\text{-}OCOH)(PMe_3)_3$ **4** and its fragments, electron populations of $Ru(H)_2(HCOOH)(PMe_3)_3$ **8** and its fragments, and the LUMO of formic acid This material is available free of charge via the Internet at http://pubs.acs.org.

JA043697N

(35) Kröcher, O.; Köppel, R. A.; Baiker, A. *Chem. Commun.* **1997**, 453.
(36) Munshi, P.; Main, A. D.; Linehan, J. C.; Tai, C.-C.; Jessop, P. G. *J. Am. Chem. Soc.* **2002**, *124*, 7963.
(37) Koike, T.; Ikariya, T. *Adv. Synth. Catal.* **2004**, *346*, 37.
(38) (a) Matsubara, T. *Organometallics* **2001**, *20*, 19. (b) Matsubara, T.; Hirao, K. *Organometallics* **2001**, *20*, 5769.